

**Characterization of Disease Course after Intramuscular or Intranasal Exposure to Sin
Nombre virus in Immunosuppressed Syrian Hamsters**

Rebecca L. Brocato^a, Jeremy J. Bearss^b, Christopher D. Hammerbeck^{a‡}, Casey C. Perley^a, Kelly
S. Stuthman^c, Nicole L. Lackemeyer^c, Steven A. Kwilas^a, and Jay W. Hooper^{a#}

^a Virology Division, United States Army Medical Research Institute of Infectious Diseases
(USAMRIID), Ft. Detrick, MD, USA

^b Pathology Division, United States Army Medical Research Institute of Infectious Diseases
(USAMRIID), Ft. Detrick, MD, USA

^c Molecular and Translational Sciences Division, United States Army Medical Research Institute
of Infectious Diseases (USAMRIID), Ft. Detrick, MD, USA

[‡] Present address: Christopher D. Hammerbeck, Bio-Techne, Minneapolis, MN

[#] Address correspondence to Jay W. Hooper, jay.w.hooper.civ@mail.mil

Running Title: SNV Disease Models in Hamsters

Key Words: Sin Nombre, hantavirus, hamster, immunosuppressed

Word count: 211 (abstract) 4,052 (text)

Summary Statement: This report describes the characterization of a small animal model that
can be utilized for the development of medical countermeasures to hantavirus disease.

ABSTRACT

Syrian hamsters exposed to Sin Nombre virus (SNV) become infected, but do not develop disease. In contrast, hamsters immunosuppressed with dexamethasone (Dex) and cyclophosphamide (CyP) and infected with SNV develop lethal disease resembling hantavirus pulmonary syndrome (HPS) in humans. Here, we provide a detailed analysis regarding the kinetics of virus dissemination after both intramuscular and intranasal challenge. Our findings revealed a ~8 day lag in the spread of virus to the lungs, kidney, liver, spleen, and heart that correlates with a delayed mean day-to-death observed when immunosuppressed hamsters are infected by the intranasal versus the intramuscular route. The length of immunosuppression with Dex and CyP required for lethal disease for intramuscular challenge was 10 days; however 19 days of treatment were required in the intranasal model. Additionally, we investigated if the steroid-sparing potential of an alternative immunosuppressive drug, mycophenolate mofetil (MMF) could replace the combination of Dex and CyP to produce lethal disease. However, MMF treatment did not increase viral replication in the lung unless it was combined with Dex. Furthermore, treatment of SNV-infected hamsters with MMF or Dex/MMF did not result in comparable lethality to hamsters administered Dex/CyP. Taken together, these experiments further refine the SNV disease model in hamsters for future use in the evaluation of medical countermeasures.

INTRODUCTION

Sin Nombre virus (SNV, genus *Hantavirus*, family *Bunaviridae*) is the predominant hantavirus in North America, and has been associated with sporadic outbreaks of lethal human disease, including the 1993 outbreak in the Four Corners region of the United States (Duchin et al., 1994) and the more recent 2012 outbreak in Yosemite National Park (Centers for Disease and Prevention, 2012). SNV is an etiological agent of hantavirus pulmonary syndrome (HPS), that is characterized in humans by leukocytosis, thrombocytopenia, and the rapid onset of acute respiratory distress (Duchin et al., 1994; Manigold and Vial, 2014). Although HPS outbreaks are isolated and sporadic, unpredictable increases in the rodent vector populations can lead to significant increases in human cases (Oliveira et al., 2016). In addition, the high case fatality rate of approximately 35% (Jonsson et al., 2010) and the absence of specific drugs or vaccines to treat or prevent HPS makes medical countermeasure development imperative. Well-

characterized animal models for the study of SNV pathogenesis will facilitate the development of medical countermeasures.

Currently, there are two SNV animal models that recapitulate human HPS disease. These are a small animal model utilizing immunosuppressed Syrian hamsters (Brocato et al., 2014) and a nonhuman primate model using virus isolated directly from the rodent host (Safronetz et al., 2014). The use of these two animal models may represent a pathway to licensure for drugs or biological products using the “Animal Rule” (21 CFR 314.600 and 21 CFR 601.90), respectively (Snoy, 2010). Therefore, continued characterization of these models enhances their potential suitability for use in drug or biological efficacy testing. In this report, we expand on our previous data set by investigating the kinetics of SNV in immunosuppressed hamsters and refine the length of immunosuppression required for disease.

Concerns over toxicity observed in lighter hamsters treated with Dex and CyP, along with an effort to reduce daily injections required with Dex/CyP treatment, led us to search for alternative immunosuppression methods. MMF (Cellcept, Genentech, Inc.), administered orally, is hydrolyzed to mycophenolic acid, an uncompetitive inhibitor of inosine monophosphate dehydrogenase that inhibits the proliferation of B and T cells (Halloran, 1996). MMF, as with most immunosuppressive drugs, was developed to prevent organ rejection following transplantation. However, MMF is also currently prescribed for the treatment of lupus as a steroid sparing drug (Kapitsinou et al., 2004). MMF is known to have reduced toxicity when compared to CyP treatment (Mok, 2016) and may be able to replicate the leukopenia that is necessary for SNV disease in hamsters (Brocato et al., 2014). Therefore, we also investigated the use of orally-administered MMF as an immunosuppressant alone and in combination with the steroid Dex in the SNV hamster disease model.

RESULTS

SNV Tissue Burden

We have previously demonstrated that hamsters immunosuppressed with Dex and CyP and infected with SNV by the intramuscular (i.m.) route develop lethal HPS disease (Brocato et al., 2014). To refine and expand this proof-of-concept work, a serial sacrifice study was performed in which immunosuppressed hamsters were infected with 2,000 PFU SNV by the i.m.

route or 4,000 PFU SNV by the intranasal (i.n.) route and then viral and immune response kinetics were analyzed every two days. The kinetics of SNV in lung, kidney, liver, spleen, and heart were determined by viral genome detection (**Fig. 1A,B**). In each of the organs tested, there was approximately a 6-8 day lag in SNV genome detection from hamsters infected by the i.n. route when compared to i.m. challenge (**Fig. 1C**).

We have previously reported on the pathology in lungs from immunosuppressed hamsters infected with SNV (Brocato et al., 2014). Here, we expand these pathology findings to the liver, kidney, spleen, and heart. Despite high viral load in these assayed organs, no significant lesions were observed by histology in liver or kidney at any timepoint (**Table S1**). Neutrophilic granulocytosis was observed in the red pulp of the spleens from immunosuppressed infected and uninfected hamsters on day 6 in SNV i.m. hamsters and days 6 and 8 on SNV i.n. hamsters. In addition, mild myocardial degeneration and necrosis was observed in the heart of 8% of infected and uninfected hamsters; this lesion was not specific to treatment group or day postinfection and likely represents a commonly described background lesion in hamsters (McInnes, 2012). Neither of these observed lesions were specifically colocalized with SNV antigen. Positive staining for SNV antigen was detected in centrilobular hepatocytes and Kupffer cells in liver tissue sections (**Fig. 2A**). Similarly, glomerular mesangial cells were positive for SNV antigen in kidney tissue sections (**Fig. 2B**), macrophages and fibroblastic reticular cells were positive in the red pulp of the spleen (**Fig. 2C**), and cardiac myocytes and capillary endothelial cells were positive in heart tissue sections (**Fig. 2D**). This observed positive staining was present in animals from both challenge routes.

The serial pathology data indicate that, regardless of challenge route, the lung is the major site of virus replication. The expression of proinflammatory and immunomodulatory cytokine-related genes and transcription factors were analyzed in lung tissue from immunosuppressed, SNV-infected (i.m.) hamsters (**Fig. 3A,B,C**). Day 0 represents data points from immunosuppressed, uninfected controls. Increased expression of the proinflammatory cytokines IL1 β and IL6, and VEGF genes were observed later in infection, and coincided with viremia in the lung (**Fig. 1A**). Increased expression of IRF2, STAT2, and iNOS were detected throughout viral infection. Expression of the IFN-stimulated genes (ISGs) protein kinase R (PKR), oligoadenylate synthetase 3 (OAS3), and IFN-induced GTP-binding protein (Mx2) were

slightly elevated at various times through the acute infection. Increased levels of expression of IFN γ and TNF α were not detected in immunosuppressed, SNV-infected hamsters. Levels of serum IFN- β were evaluated in immunocompetent and immunosuppressed hamsters infected with SNV. There was a significant reduction in IFN- β expression in infected hamsters treated with Dex and CyP 2 days postinfection ($p < 0.0001$). However, IFN- β expression levels between untreated or Dex/CyP-treated animals were not statistically significant by days 4 and 6 postinfection (**Fig. 3D**).

Optimization of SNV/Hamster Disease Models

To evaluate the length of immunosuppression required for SNV-induced HPS, hamsters were pretreated with a combination of Dex and CyP beginning on day -3 and immunosuppression with Dex and CyP was stopped at various time points postinfection. On day 0, hamsters were challenged with 2,000 PFU by the i.m. route. Immunosuppression through day 7 postinfection resulted in significant lethality (day 7, $p < 0.0001$, day 10, $p = 0.0024$, day 13, $p = 0.0085$) (**Fig. 4A**). In contrast, immunosuppression through day 5 postinfection did not produce uniform disease, but did result in a statistically significant 63% lethality ($p = 0.0133$) compared to untreated, infected hamsters. In surviving hamsters, day 28 (end of study) lung tissue was evaluated for SNV genome by RT-PCR. Hamsters treated with Dex and CyP had elevated levels of SNV present in the lungs when compared to untreated, infected controls (**Fig. 4B**).

Using immunosuppression beginning on day -3 through day 7 postinfection, a 50% lethal dose (LD50) experiment was performed to determine the SNV dose necessary for hamsters to develop HPS. As little as 2 PFU SNV resulted in lethal disease in 50% of the animals in that group (**Fig. 4C**) when hamsters were challenged by the i.m. route. Statistical analysis determined that the LD50 dosage is 2.5 PFU for this model. Hamster groups challenged with 20, 200, and 2,000 PFU SNV all exhibited statistically significant increases in lethality when compared to uninfected hamsters ($p = 0.0243$, $p = 0.0020$, and $p = 0.0020$, respectively). Lung tissue collected on day 28 from surviving animals demonstrate the presence of SNV genome in treated, infected hamsters (**Fig. 4D**).

For the SNV i.n. model, the length of immunosuppression with Dex and CyP was determined by truncating immunosuppression to 13 and 16 days postinfection. When challenged with 4,000 PFU SNV, only 12.5% of hamsters receiving Dex and CyP through day 13 developed lethal disease. However, 87.5% of hamsters receiving Dex and CyP through day 16 developed lethal disease resulting in a statistically significant reduction in survival ($p=0.0012$) (**Fig. 5A**). Of the 7 surviving hamsters on day 28 (end of study), results of a nucleocapsid (N)-ELISA assay indicate that 6 of the hamsters immunosuppressed to day 13 developed an antibody response to SNV and the lone survivor from the Dex/CyP treatment through day 16 did not develop an antibody response to SNV above the limit of detection for the assay (**Fig. 5B**). Hamsters that developed lethal disease had approximately 10^5 molecules of small (S)-segment genome in the lung (**Fig. 5C**). Hamsters surviving to day 28 had comparable levels of S-segment genome in lung tissue; however, hamsters not receiving Dex and CyP developed an increased antibody response to SNV infection when compared to hamsters receiving Dex and CyP through day 13, although not statistically significant. There is not a direct correlation between the S-segment genome detected and the magnitude of the antibody response as measured by N-ELISA. However, the results of this experiment do support the hypothesis that longer immunosuppression, through day 16 postinfection, is required to allow i.n. instilled SNV to develop pathogenic disease in hamsters.

Alternative Immunosuppression Approach

The impact of replacing CyP with MMF was evaluated in SNV infection in hamsters. Hamsters were immunosuppressed with either a combination of Dex and CyP, CyP alone, a combination of Dex and MMF, MMF alone, or administered no immunosuppressive treatment beginning on day -3 prior to infection through day 10 postinfection. All hamsters treated with MMF were administered a dosage of 30 mg/kg/day. Immunosuppression with the combination of Dex and CyP provided the greatest lethality (86%, $p=0.0029$ when compared to no treatment controls) (**Fig. 6A**), followed by immunosuppression with CyP alone (57%, $p=0.0346$ when compared to no treatment controls) thereby confirming our previous report (Brocato et al., 2014). Immunosuppression with the combination of Dex and MMF or MMF alone resulted in 12% and 0% lethality, respectively. In addition, immunosuppression using solely MMF did not reduce WBCs (**Fig. 6B**). Lung tissue collected from a subset of animals on day 12 postinfection

demonstrates that Dex administered in combination with either CyP or MMF is required for a statistically significant increase in SNV genome over No Treatment controls ($p=0.0219$ and $p=0.0089$, respectively) (**Fig. 6C**). Correspondingly, the Dex/CyP and Dex/MMF groups had notable interstitial inflammation in the day 12 lung tissue (3/3 hamsters in both groups), more so than groups receiving CyP or MMF alone, or left untreated (2/3, 2/3, and 0/3 hamsters per group, respectively) (data not shown). RNA analysis of lung homogenates collected from surviving animals on day 28 postinfection also supports the requirement for including Dex in a combination treatment (**Fig. 6D**). Furthermore, results of an N-ELISA conducted with sera from surviving hamsters on day 28 postinfection show that the ability of hamsters to develop SNV-specific antibodies is reduced in hamsters immunosuppressed with CyP (alone [$p=0.0179$ when compared to no treatment controls] or in combination with Dex) but not MMF (alone or in combination with Dex) (**Fig. 6E**).

Increased dosages of MMF were evaluated in uninfected hamsters to determine if a higher concentration could reduce WBCs to levels observed in Dex/CyP treatment. Hamsters were treated with MMF at concentrations ranging from 30-360 mg/kg for two days by the oral route. On the third day, hematology analysis was conducted. The results of this dosing study indicate that even a >10-fold increase in MMF was not able to significantly reduce WBCs when compared to no treatment controls (**Fig. 7**).

DISCUSSION

Animal models are an essential component for elucidating viral pathogenesis, testing and evaluating vaccines, antivirals, and biologicals, and the potential licensing of those products. Our first report on the SNV/immunosuppressed hamster model focused mainly on the disease in the target organ (i.e. lung) (Brocato et al., 2014); in the current study we demonstrate that SNV disseminates to other organs, namely the kidney, liver, spleen, and heart. Others have demonstrated that dissemination can occur after serially passaging SNV through immunocompetent Syrian hamsters (Safronetz et al., 2013b); here we demonstrate that this dissemination can be replicated with low-passage cell culture virus in immunosuppressed hamsters. Similar to immunocompetent hamsters infected by Andes virus (ANDV) by the i.m. route (Wahl-Jensen et al., 2007), there is an approximate 6 day incubation period before viremia can be detected in immunosuppressed hamsters infected with SNV by the i.m. route. A 6-8 day

201 delay in viremia is observed when comparing the SNV/immunosuppressed i.m. and i.n. routes of
202 infection. A similar delay in death is observed between these two routes for ANDV infection in
203 hamsters (Hooper et al., 2008). These ANDV/hamster models have been used to demonstrate
204 that antivirals such as ribavirin, favipiravir, and neutralizing antibodies are only efficacious if
205 administered prior to the detection of viremia (Haese et al., 2015; Hooper et al., 2014; Hooper et
206 al., 2008; Ogg et al., 2013; Safronetz et al., 2013a). Efforts to expand this therapeutic window
207 have been largely unsuccessful. The SNV/immunosuppressed hamster model provides an
208 alternative small animal model for the evaluation of similar candidate medical countermeasures
209 against another important virus that causes HPS.

210 Viruses have evolved multiple mechanisms for subverting the host immune response
211 (Rouse and Horohov, 1986). ANDV modulation of early host innate responses both *in vivo*
212 (Safronetz et al., 2011) and *in vitro* (Levine et al., 2010) may contribute to the establishment of
213 the infection and the associated pathogenicity observed in the hamster model. The lack of disease
214 associated with SNV infection in immunocompetent hamsters may indicate that, unlike ANDV,
215 SNV is unable to modulate early innate responses. We hypothesize that dissemination of SNV
216 and pathogenicity in immunosuppressed hamsters is caused by modulation of early host innate
217 responses and a subsequent inability of the adaptive immune response to contain and clear
218 infection. We further speculate that the timing of the immune response to virus infection is
219 critical to result in an asymptomatic infection or death of the hamster. Negative regulation of
220 transcription factors AP-1 and NF- κ B by Dex treatment suppresses cytokines and chemokines
221 such as IL-2, IL-6, IFN- γ , and IL-8 (Karin, 1998). In addition, glucocorticoid treatment has been
222 shown to inhibit signaling by cytokines that utilize the Jak-STAT pathway, namely IL-2 and IL-
223 12 (Hu et al., 2003). In the current study, hamsters treated with Dex did not have early increased
224 expression of these cytokines and chemokines. Expression of IL-6 later in infection is also
225 observed in human HPS cases (Borges et al., 2008; Morzunov et al., 2015) and represents the
226 hamsters' ability to initiate a proinflammatory response despite Dex treatment. VEGF and IL-6
227 promote migration of mononuclear cells to the lung and these cells are observed in the
228 histological analysis of lung sections from SNV-infected, immunosuppressed hamsters (Brocato
229 et al., 2014). The lack of STAT1 upregulation, impacted by Dex treatment (Bhattacharyya et al.,
230 2011), contributes to the suppression of IFN- γ (Hu et al., 2003), similar to the expression levels
231 of STAT1 and IFN- γ presented herein. Similarly, a reduction in IFN- β expression at short

timepoints after SNV challenge (i.e. 2 days) likely contributes to increased SNV dissemination and pathogenicity in immunosuppressed hamsters compared to immunocompetent hamsters. The ANDV N has been shown to inhibit type I IFN signaling responses whereas SNV N does not (Cimica et al., 2014). Treatment of hamsters with Dex may allow SNV to replicate in this host in a manner similar to ANDV infection of immunocompetent hamsters.

SNV readily infects hamsters with a 50% infectious dose (ID₅₀) of less than 2 PFU (Hooper et al., 2001). When hamsters are immunosuppressed from day -3 to 7 days postinfection and infected with SNV by the i.m. route, an LD₅₀ dosage of 2.5 PFU was calculated. Thus, the ability to infect hamsters appears to be very efficient regardless of whether the hamster is immunosuppressed or not. These optimization experiments demonstrate the balance of the length of immunosuppression required and challenge dose for a uniformly lethal model for the i.m. and i.n. routes of exposure.

MMF has recently been accepted as a treatment to patients suffering from lupus nephritis, as an alternative to CyP or CyP combined with a glucocorticoid (Tesar, 2016). By replacing CyP with MMF in the SNV/hamster model, we evaluated the steroid sparing potential of MMF. This experiment was rationalized by the possibility of administering a single drug, and the ability to compound this drug into the feed for future experiments. A hallmark of the Dex/CyP model is pronounced leukopenia resulting in a diminution of adaptive and innate immune responses that allow SNV to replicate and cause acute disease. However, hamsters treated with MMF alone did not exhibit the reduction in WBCs observed with CyP treatment, nor allow SNV to replicate in the lung to levels observed when Dex was incorporated in the treatment regimen. Immunosuppressive drugs were administered through day 10 postinfection. This timepoint was selected from the truncated immunosuppression experiment (**Fig. 4A**) demonstrating that Dex/CyP treatment through day 10 resulted in 100% lethality. A single death was observed in the Dex/MMF treatment group leading us to hypothesize that potentially extending the treatment regimen beyond day 10 may have resulted in increased lethality. Increased concentrations of MMF did not reduce WBCs in treated hamsters (**Fig. 7**); whether this is a species-specific phenomenon or a higher dosage of MMF is needed to induce leukopenia is currently unknown. Future efforts will utilize the combination of Dex and CyP in the SNV/hamster model.

The SNV/immunosuppressed hamster model represents an alternative small animal lethal disease model that recapitulates many of the salient features of the ANDV/hamster model and human HPS disease. Further refinement of this model allows the testing of vaccines and medical countermeasures to combat hantavirus disease and may provide an alternative animal model for licensure of products under the FDAs “Animal Rule.”

MATERIALS AND METHODS

Viruses, cells, and medium. SNV strain CC107 (Schmaljohn et al., 1995) was propagated in Vero E6 cells (Vero C1008, ATCC CRL 1586). Preparation of twice plaque-purified SNV stock has been described previously (Hooper et al., 2001). Cells were maintained in Eagle’s minimum essential medium with Earle’s salts containing 10% fetal bovine serum, 10 mM HEPES, pH 7.4, and Penicillin Streptomycin (Invitrogen) at 1X, and gentamicin sulfate (50 µg/ml) at 37°C in a 5% CO₂ incubator.

Dex, CyP, and MMF administration. Water soluble Dex and CyP monohydrate were purchased from Sigma-Aldrich. MMF was purchased from Selleck Chemicals. On the indicated days, anesthetized hamsters were injected intraperitoneally (i.p.) with the indicated dosages per body weight of drug diluted in sterile phosphate-buffered saline (PBS), pH 7.4. Hamsters were treated with a loading dose of 16 mg/kg Dex and 140 mg/kg CyP on day -3, 8 mg/kg Dex on day -2, 8 mg/kg Dex and 100 mg/kg CyP on day -1, 4 mg/kg Dex on days 0, 2, 3, 5, 6, 8, 9, 11, 12, 13, 15, 16, 17, 19, 20, 21, and 4 mg/kg Dex and 100 mg/kg CyP on days 1, 4, 7, 10, 14, 18, and 22. Each experiment specifies the length of Dex and CyP immunosuppression administered to animals. Hamsters were administered 30 mg/kg MMF by the oral route daily from day -3 to day 10 postinfection (**Fig. 6**). Hamsters were administered 30-360 mg/kg MMF by the oral route for 2 days prior to hematology (**Fig. 7**).

Challenge with hantavirus. Female Syrian hamsters 6-8 wks of age and > 100g (Envigo, Indianapolis, IN) were anesthetized by inhalation of vaporized isoflurane using an IMPAC 6 veterinary anesthesia machine. Once anesthetized, hamsters were injected with the indicated concentration of virus diluted in PBS. Intramuscular (i.m.) (caudal thigh) injections consisted of 0.2ml delivered with a 1ml syringe with a 25-gauge, 5/8in needle. Intranasal (i.n.) instillation consisted of 50µl total volume delivered as 25µl per nare with a plastic pipette tip. Groups of 8

hamsters were typically used for experimental treatments, unless otherwise stated. All work involving hamsters was performed in an animal biosafety level 4 (ABSL-4) laboratory. Euthanasia was performed on animals meeting early endpoint criteria.

ELISA. The enzyme-linked immunosorbent assay (ELISA) used to detect N-specific antibodies (N-ELISA) was described previously (Elgh et al., 1997; Hooper et al., 1999). The endpoint titer was determined as the highest dilution that had an optical density (OD) greater than the mean OD for serum samples from negative-control wells plus 3 standard deviations. The Puumala N antigen was used to detect SNV N-specific antibodies as previously reported (Xiao et al., 1993). Hamster-specific IFN- β ELISA (MyBiosource, San Diego, CA) was run according to manufacturer's published protocols.

Isolation of RNA and real-time PCR. Approximately 250 mg of organ tissue was homogenized in 1.0 ml TRIzol reagent using gentleMACS M tubes and a gentleMACS dissociator on the RNA setting. RNA was extracted from TRIzol samples as recommended by the manufacturer. The concentration of the extracted RNA was determined using a NanoDrop 8000 instrument and raised to a final concentration of 10 ng/ μ l. Real-time PCR was conducted on a BioRad CFX thermal cycler using an Invitrogen Power SYBR Green RNA-to-Ct one-step kit according to the manufacturer's protocols. Primer sequences are SNV S 26F 5'-CTA CGA CTA AAG CTG GAA TGA GC-3' and SNV S 96R 5'-GAG TTG TTG TTC GTG GAG AGT G-3' (Trombley et al., 2010). Cycling conditions were 30 min at 48°C, 10 min at 95°C, followed by 40 cycles of 15 sec at 95°C and 1 min at 60°C. Data acquisition occurs following the annealing step.

Host responses were monitored using hamster-specific primers for IL1 β , IL2, IL6, IL10, IL12p35, IRF1, IRF2, IFN γ , iNOS, Mx2, OAS3, PKR, STAT1, STAT2, TNF α , and VEGF (Toth et al., 2015; Zivcec et al., 2011) using HPRT as an internal control. Data was analyzed using the $\Delta\Delta$ Ct method (Livak and Schmittgen, 2001) where the Ct was first normalized to the internal control and then compared to an immunosuppressed, mock-treated animal.

Hematology. Blood samples collected in lithium heparin capillary blood collection tubes were analyzed using an Advia 120 hematology analyzer using proprietary software version 3.1.8.0-MS. The dog setting was used for the complete blood count and guinea pig setting was used for the differential.

Preparation of tissues for histology. Tissues were fixed in 10% neutral-buffered formalin for ≥ 21 days. Tissues were then trimmed, processed under vacuum through increasing concentrations of alcohols, and embedded in paraffin. 5-6 μm sections of paraffin embedded tissue were cut and mounted on glass slides, stained with hematoxylin-eosin (H&E), and mounted under a glass coverslip for histologic evaluation. Immunolocalization of SNV in tissues was performed with an immunoperoxidase procedure (horseradish peroxidase EnVision system; Dako) according to the manufacturer's directions. The primary antibody was an α -SNV nucleocapsid rabbit polyclonal antibody diluted 1:3,000 (provided by Diagnostic Service Division, USAMRIID). Negative controls included naïve hamster tissue incubated with nonimmune rabbit IgG in place of the primary antibody and naïve hamster tissue exposed to the primary antibody and negative serum. After deparaffinization and peroxidase blocking, tissue sections were pretreated with proteinase K for 6 min at room temperature, rinsed, and then covered with primary antibody and incubated at room temperature for 1 hr. They were rinsed, and then the peroxidase-labeled polymer (secondary antibody) was applied for 30 min. Slides were rinsed, and a substrate-chromogen solution (3,3'-diaminobenzidine; Dako) was applied for 5 min. The substrate-chromogen solution was rinsed off the slides, and the slides were stained with hematoxylin and rinsed. The sections were dehydrated and cleared with xyless, and then a coverslip was placed.

Statistical analysis. Survival curves were compared with Kaplan-Meier survival analysis with log-rank comparisons and Dunnett correction. A Bayesian probit model was used to estimate 95% highest posterior density intervals for a 50% lethal dose calculation. Comparison of viral genome results was done using a one-way ANOVA with Dunnett's multiple comparison test. Comparison of WBC was done using a paired t test. Comparison of N-ELISA was done using Mann-Whitney test. *P* values of less than 0.05 were considered significant. Analyses were conducted using GraphPad Prism (version 6); Bayesian analyses were performed using Stan 2.1.0.

Ethics statement. Animal research was conducted under an IACUC approved protocol at USAMRIID (USDA Registration Number 51-F-00211728 & OLAW Assurance number A3473-01) in compliance with the Animal Welfare Act and other federal statutes and regulations relating to animals and experiments involving animals. The facility where this research was

conducted is fully accredited by the Association for Assessment and Accreditation of Laboratory Animal Care, International and adheres to principles stated in the Guide for the Care and Use of Laboratory Animals, National Research Council, 2011.

FIGURE LEGENDS

Figure 1. SNV kinetics in Syrian hamster organs. Three hamsters from each of the immunosuppressed, SNV i.m. and i.n. groups were euthanized at each timepoint. Tissues were excised, homogenized, and RNA isolated for SNV genome detection by RT-PCR. SNV S-segment kinetics was measured in lungs, kidneys, livers, spleens, and hearts in hamsters infected by the **A)** i.m. route and **B)** i.n. route. Mean values and \pm SD are shown. **C)** SNV genome organ burden is shown as the mean of all organs evaluated from all animals at each timepoint. The lag in SNV genome organ burden between the two routes of infection is shown as the blue arrow. A single hamster on day 12 from the Dex/CyP SNV i.n. group is shown separately as an outlier depicted by the filled triangle (\blacktriangle).

Figure 2. SNV antigen detection in hamster organs by immunohistochemistry.

Immunohistochemistry using an α -nucleocapsid antibody was performed on **A)** liver tissue, **B)** kidney tissue, **C)** spleen tissue, and **D)** heart tissue from immunosuppressed, SNV-infected hamsters collected on either day 10 (liver, kidney, and heart) or day 20 (spleen) postinfection. **A,** **B,** **C,** 400X magnification. **D,** 200X magnification. Size bars are indicated in each panel.

Figure 3. Normalized fold expression of select cytokines in lung tissue of

immunosuppressed, SNV-infected hamsters. **A, B, C)** RNA from homogenized lung tissue was isolated from immunosuppressed, SNV i.m. hamsters (n=3 per timepoint). Gene regulation was normalized to the reference gene HPRT and compared using the $\Delta\Delta$ Ct method on the indicated days. Individual values are shown with the horizontal line representing the mean. **D)** Serum IFN- β levels from SNV-infected and immunosuppressed, SNV-infected hamsters analyzed by ELISA. ***, $P < 0.001$; ns, not significant.

Figure 4. Optimization of immunosuppressed SNV i.m. model. **A)** The length of

immunosuppression with Dex and CyP required for the development of lethal HPS was determined in groups of 7 or 8 hamsters each. Hamsters were challenged with 2,000 PFU i.m. and immunosuppression beginning on day -3 was truncated to days 5, 7, 10, and 13 days

postinfection. Hamsters were monitored for survival. **B)** Lung tissues collected from surviving hamsters (day 28) were analyzed for the presence of SNV genome by RT-PCR. **C)** Groups of 10 hamsters each were immunosuppressed with Dex and CyP from day -3 through day 7 postinfection. Hamsters were challenged with the indicated concentration of virus on day 0 and monitored for survival. **D)** Lung tissues collected from surviving hamsters (day 28) were analyzed for the presence of SNV genome by RT-PCR. *, $P < 0.05$; **, $P < 0.01$; ***, $P < 0.001$.

Figure 5. Optimization of immunosuppressed SNV i.n. model. **A)** Groups of 8 hamsters each were immunosuppressed with Dex and CyP beginning on day -3 through the indicated day. All hamsters were infected with 4,000 PFU SNV by the i.n. route and monitored for survival. **B)** Sera from surviving hamsters on day 35 were analyzed by N-ELISA. **C)** Lung tissues collected after the onset of HPS (blue circles indicate hamsters were euthanized or found dead) or on day 35 postinfection were analyzed for the presence of SNV genome by RT-PCR. **, $P < 0.01$.

Figure 6. Alternative immunosuppression of hamsters using MMF. Groups of 6-8 hamsters each were immunosuppressed with CyP, Dex and CyP, MMF, Dex and MMF, or left untreated beginning on day -3 through day 10 postinfection. All hamsters were infected with 2,000 PFU SNV by the i.m. route on day 0. Hamsters were monitored for **A)** survival and **B)** WBCs. **C)** A subset of hamsters not used for survival were euthanized on day 12 and lung homogenates analyzed for SNV genome by RT-PCR. Hamsters surviving to day 28 were euthanized and **D)** lung homogenates analyzed for SNV genome by RT-PCR and **E)** serum analyzed by N-ELISA. *, $P < 0.05$; **, $P < 0.01$; ***, $P < 0.001$; ns, not significant.

Figure 7. Dose optimization of MMF in hamsters. Groups of 3 hamsters each were administered increasing concentrations of MMF for two days by the oral route. Whole blood collected on day 3 was analyzed for WBCs.

ACKNOWLEDGEMENTS

We thank the USAMRIID Veterinary Medical Division and Chris Mech for technical assistance, Steven Kern for statistical analyses, and Joseph Golden for critical review of the manuscript.

Research reported in this publication was supported by the National Institute of Allergy and Infectious Diseases of the National Institutes of Health under Award Number R01AI098933. Opinions, interpretations, conclusions, and recommendations are ours and are not necessarily endorsed by the U.S. Army or the Department of Defense. No competing interests declared.

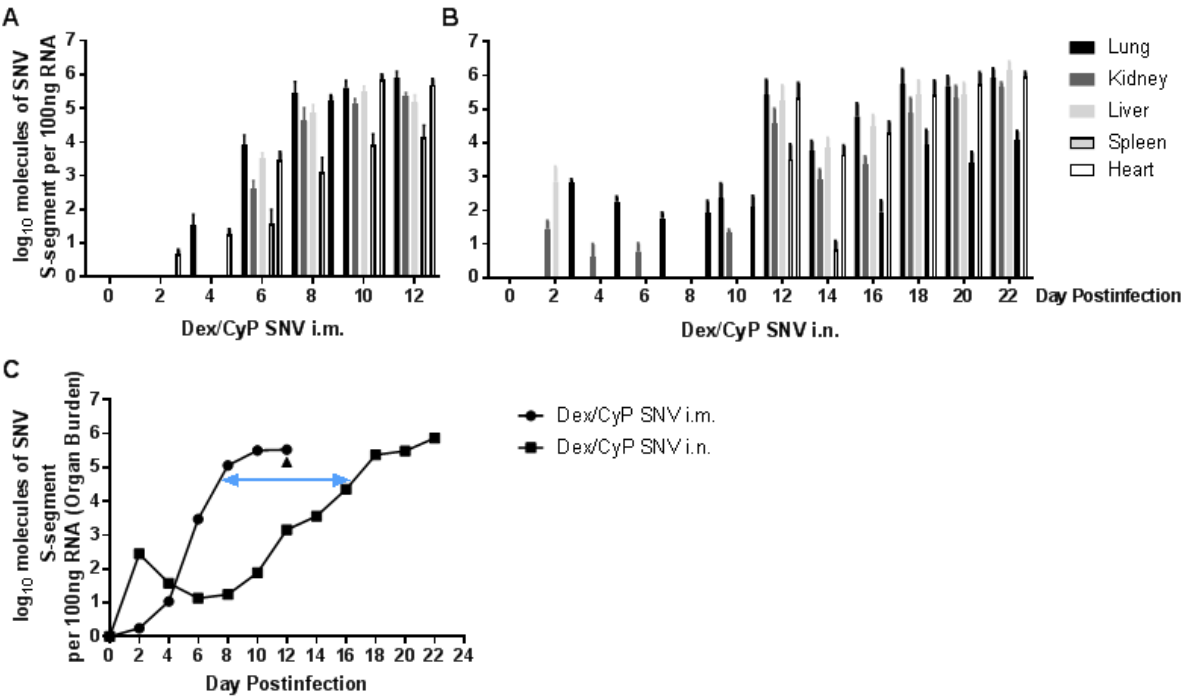
REFERENCES

- Bhattacharyya, S., Zhao, Y., Kay, T. W. and Muglia, L. J.** (2011). Glucocorticoids target suppressor of cytokine signaling 1 (SOCS1) and type 1 interferons to regulate Toll-like receptor-induced STAT1 activation. *Proc Natl Acad Sci U S A* **108**, 9554-9.
- Borges, A. A., Campos, G. M., Moreli, M. L., Moro Souza, R. L., Saggioro, F. P., Figueiredo, G. G., Livonesi, M. C. and Moraes Figueiredo, L. T.** (2008). Role of mixed Th1 and Th2 serum cytokines on pathogenesis and prognosis of hantavirus pulmonary syndrome. *Microbes Infect* **10**, 1150-7.
- Brocato, R. L., Hammerbeck, C. D., Bell, T. M., Wells, J. B., Queen, L. A. and Hooper, J. W.** (2014). A lethal disease model for hantavirus pulmonary syndrome in immunosuppressed Syrian hamsters infected with Sin Nombre virus. *J Virol* **88**, 811-9.
- Centers for Disease, C. and Prevention.** (2012). Hantavirus pulmonary syndrome in visitors to a national park--Yosemite Valley, California, 2012. *MMWR Morb Mortal Wkly Rep* **61**, 952.
- Cimica, V., Dalrymple, N. A., Roth, E., Nasonov, A. and Mackow, E. R.** (2014). An innate immunity-regulating virulence determinant is uniquely encoded by the Andes virus nucleocapsid protein. *MBio* **5**.
- Duchin, J. S., Koster, F. T., Peters, C. J., Simpson, G. L., Tempest, B., Zaki, S. R., Ksiazek, T. G., Rollin, P. E., Nichol, S., Umland, E. T. et al.** (1994). Hantavirus pulmonary syndrome: a clinical description of 17 patients with a newly recognized disease. The Hantavirus Study Group. *N Engl J Med* **330**, 949-55.
- Elgh, F., Lundkvist, A., Alexeyev, O. A., Stenlund, H., Avsic-Zupanc, T., Hjelle, B., Lee, H. W., Smith, K. J., Vainionpaa, R., Wiger, D. et al.** (1997). Serological diagnosis of hantavirus infections by an enzyme-linked immunosorbent assay based on detection of immunoglobulin G and M responses to recombinant nucleocapsid proteins of five viral serotypes. *J Clin Microbiol* **35**, 1122-30.
- Haese, N., Brocato, R. L., Henderson, T., Nilles, M. L., Kwilas, S. A., Josleyn, M. D., Hammerbeck, C. D., Schiltz, J., Royals, M., Ballantyne, J. et al.** (2015). Antiviral Biologic Produced in DNA Vaccine/Goose Platform Protects Hamsters Against Hantavirus Pulmonary Syndrome When Administered Post-exposure. *PLoS Negl Trop Dis* **9**, e0003803.
- Halloran, P. F.** (1996). Molecular mechanisms of new immunosuppressants. *Clin Transplant* **10**, 118-23.
- Hooper, J. W., Brocato, R. L., Kwilas, S. A., Hammerbeck, C. D., Josleyn, M. D., Royals, M., Ballantyne, J., Wu, H., Jiao, J. A., Matsushita, H. et al.** (2014). DNA vaccine-derived human IgG produced in transchromosomal bovines protect in lethal models of hantavirus pulmonary syndrome. *Sci Transl Med* **6**, 264ra162.

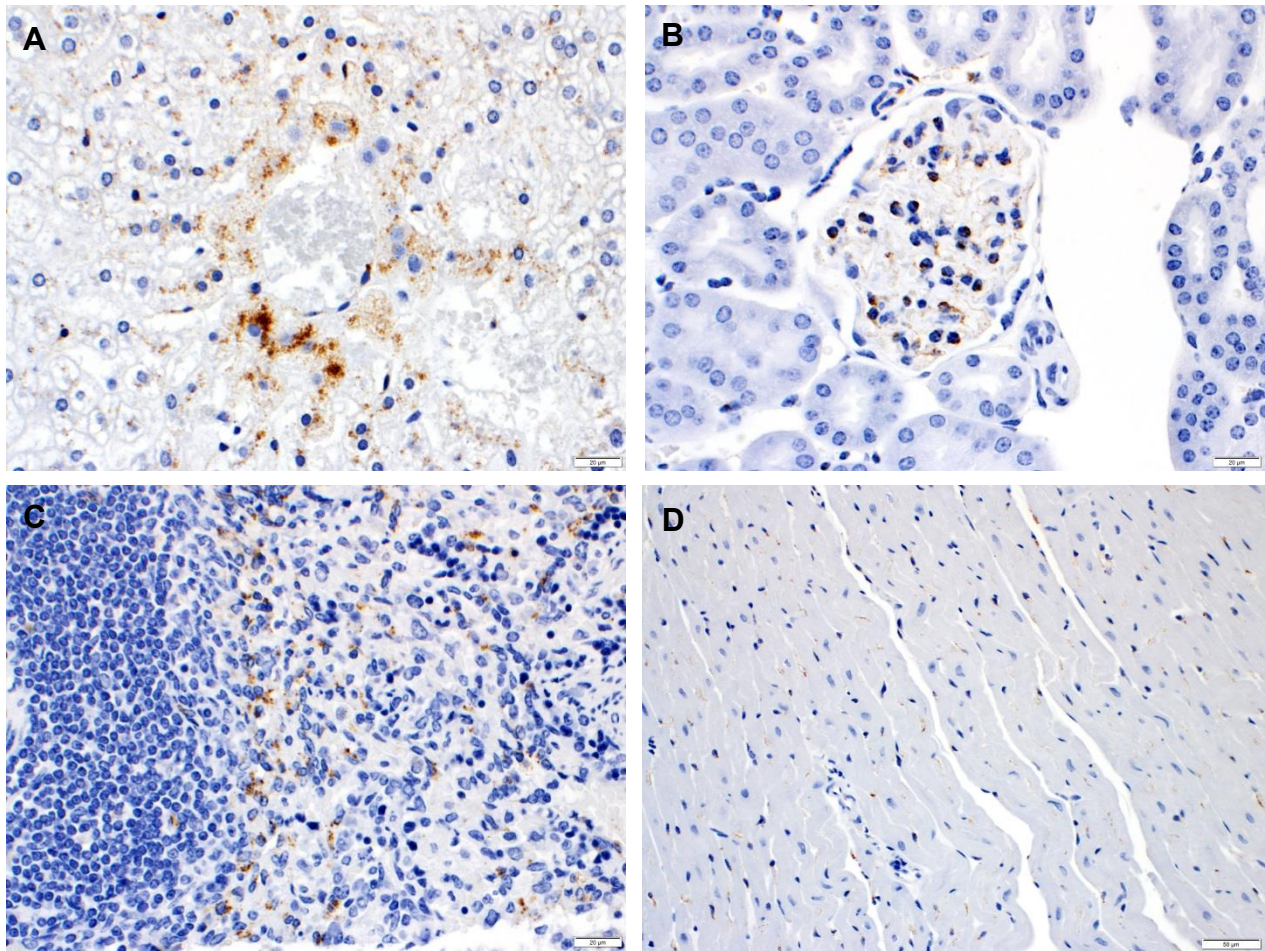
- 447 **Hooper, J. W., Ferro, A. M. and Wahl-Jensen, V.** (2008). Immune serum produced by
448 DNA vaccination protects hamsters against lethal respiratory challenge with Andes virus. *J Virol*
449 **82**, 1332-8.
- 450 **Hooper, J. W., Kamrud, K. I., Elgh, F., Custer, D. and Schmaljohn, C. S.** (1999).
451 DNA vaccination with hantavirus M segment elicits neutralizing antibodies and protects against
452 seoul virus infection. *Virology* **255**, 269-78.
- 453 **Hooper, J. W., Larsen, T., Custer, D. M. and Schmaljohn, C. S.** (2001). A lethal
454 disease model for hantavirus pulmonary syndrome. *Virology* **289**, 6-14.
- 455 **Hu, X., Li, W. P., Meng, C. and Ivashkiv, L. B.** (2003). Inhibition of IFN-gamma
456 signaling by glucocorticoids. *J Immunol* **170**, 4833-9.
- 457 **Jonsson, C. B., Figueiredo, L. T. and Vapalahti, O.** (2010). A global perspective on
458 hantavirus ecology, epidemiology, and disease. *Clin Microbiol Rev* **23**, 412-41.
- 459 **Kapitsinou, P. P., Boletis, J. N., Skopouli, F. N., Boki, K. A. and Moutsopoulos, H.**
460 **M.** (2004). Lupus nephritis: treatment with mycophenolate mofetil. *Rheumatology (Oxford)* **43**,
461 377-80.
- 462 **Karin, M.** (1998). New twists in gene regulation by glucocorticoid receptor: is DNA
463 binding dispensable? *Cell* **93**, 487-90.
- 464 **Levine, J. R., Prescott, J., Brown, K. S., Best, S. M., Ebihara, H. and Feldmann, H.**
465 (2010). Antagonism of type I interferon responses by new world hantaviruses. *J Virol* **84**, 11790-
466 801.
- 467 **Livak, K. J. and Schmittgen, T. D.** (2001). Analysis of relative gene expression data
468 using real-time quantitative PCR and the 2(-Delta Delta C(T)) Method. *Methods* **25**, 402-8.
- 469 **Manigold, T. and Vial, P.** (2014). Human hantavirus infections: epidemiology, clinical
470 features, pathogenesis and immunology. *Swiss Med Wkly* **144**, w13937.
- 471 **McInnes, E. F.** (2012). Chapter 5: Hamsters and Other Rodents. In *Background Lesions*
472 *in Laboratory Animals*, pp. 73-79. Edinburgh: Saunders-Elsevier.
- 473 **Mok, C. C.** (2016). Con: Cyclophosphamide for the treatment of lupus nephritis. *Nephrol*
474 *Dial Transplant* **31**, 1053-7.
- 475 **Morzunov, S. P., Khaiboullina, S. F., St Jeor, S., Rizvanov, A. A. and Lombardi, V.**
476 **C.** (2015). Multiplex Analysis of Serum Cytokines in Humans with Hantavirus Pulmonary
477 Syndrome. *Front Immunol* **6**, 432.
- 478 **Ogg, M., Jonsson, C. B., Camp, J. V. and Hooper, J. W.** (2013). Ribavirin protects
479 Syrian hamsters against lethal hantavirus pulmonary syndrome--after intranasal exposure to
480 Andes virus. *Viruses* **5**, 2704-20.
- 481 **Oliveira, R. C., Sant'ana, M. M., Guterres, A., Fernandes, J., Hillesheim, N. L.,**
482 **Lucini, C., Gomes, R., Lamas, C., Bochner, R., Zeccer, S. et al.** (2016). Hantavirus pulmonary
483 syndrome in a highly endemic area of Brazil. *Epidemiol Infect* **144**, 1096-106.
- 484 **Rouse, B. T. and Horohov, D. W.** (1986). Immunosuppression in viral infections. *Rev*
485 *Infect Dis* **8**, 850-73.
- 486 **Safronetz, D., Falzarano, D., Scott, D. P., Furuta, Y., Feldmann, H. and Gowen, B.**
487 **B.** (2013a). Antiviral efficacy of favipiravir against two prominent etiological agents of
488 hantavirus pulmonary syndrome. *Antimicrob Agents Chemother* **57**, 4673-80.
- 489 **Safronetz, D., Prescott, J., Feldmann, F., Haddock, E., Rosenke, R., Okumura, A.,**
490 **Brining, D., Dahlstrom, E., Porcella, S. F., Ebihara, H. et al.** (2014). Pathophysiology of
491 hantavirus pulmonary syndrome in rhesus macaques. *Proc Natl Acad Sci U S A* **111**, 7114-9.

- 492 **Safronetz, D., Prescott, J., Haddock, E., Scott, D. P., Feldmann, H. and Ebihara, H.**
 493 (2013b). Hamster-adapted Sin Nombre virus causes disseminated infection and efficiently
 494 replicates in pulmonary endothelial cells without signs of disease. *J Virol* **87**, 4778-82.
- 495 **Safronetz, D., Zivcec, M., Lacasse, R., Feldmann, F., Rosenke, R., Long, D.,**
 496 **Haddock, E., Brining, D., Gardner, D., Feldmann, H. et al.** (2011). Pathogenesis and host
 497 response in Syrian hamsters following intranasal infection with Andes virus. *PLoS Pathog* **7**,
 498 e1002426.
- 499 **Schmaljohn, A. L., Li, D., Negley, D. L., Bressler, D. S., Turell, M. J., Korch, G. W.,**
 500 **Ascher, M. S. and Schmaljohn, C. S.** (1995). Isolation and initial characterization of a
 501 newfound hantavirus from California. *Virology* **206**, 963-72.
- 502 **Snoy, P. J.** (2010). Establishing efficacy of human products using animals: the US food
 503 and drug administration's 'animal rule'. *Veterinary Pathology* **47**, 774-778.
- 504 **Tesar, V.** (2016). Moderator's view: Cyclophosphamide in lupus nephritis. *Nephrol Dial*
 505 *Transplant* **31**, 1058-61.
- 506 **Toth, K., Lee, S. R., Ying, B., Spencer, J. F., Tollefson, A. E., Sagartz, J. E., Kong, I.**
 507 **K., Wang, Z. and Wold, W. S.** (2015). STAT2 Knockout Syrian Hamsters Support Enhanced
 508 Replication and Pathogenicity of Human Adenovirus, Revealing an Important Role of Type I
 509 Interferon Response in Viral Control. *PLoS Pathog* **11**, e1005084.
- 510 **Trombley, A. R., Wachter, L., Garrison, J., Buckley-Beason, V. A., Jahrling, J.,**
 511 **Hensley, L. E., Schoepp, R. J., Norwood, D. A., Goba, A., Fair, J. N. et al.** (2010).
 512 Comprehensive panel of real-time TaqMan polymerase chain reaction assays for detection and
 513 absolute quantification of filoviruses, arenaviruses, and New World hantaviruses. *Am J Trop*
 514 *Med Hyg* **82**, 954-60.
- 515 **Wahl-Jensen, V., Chapman, J., Asher, L., Fisher, R., Zimmerman, M., Larsen, T.**
 516 **and Hooper, J. W.** (2007). Temporal analysis of Andes virus and Sin Nombre virus infections
 517 of Syrian hamsters. *J Virol* **81**, 7449-62.
- 518 **Xiao, S. Y., Spik, K. W., Li, D. and Schmaljohn, C. S.** (1993). Nucleotide and deduced
 519 amino acid sequences of the M and S genome segments of two Puumala virus isolates from
 520 Russia. *Virus Res* **30**, 97-103.
- 521 **Zivcec, M., Safronetz, D., Haddock, E., Feldmann, H. and Ebihara, H.** (2011).
 522 Validation of assays to monitor immune responses in the Syrian golden hamster (*Mesocricetus*
 523 *auratus*). *J Immunol Methods* **368**, 24-35.

Figure 1



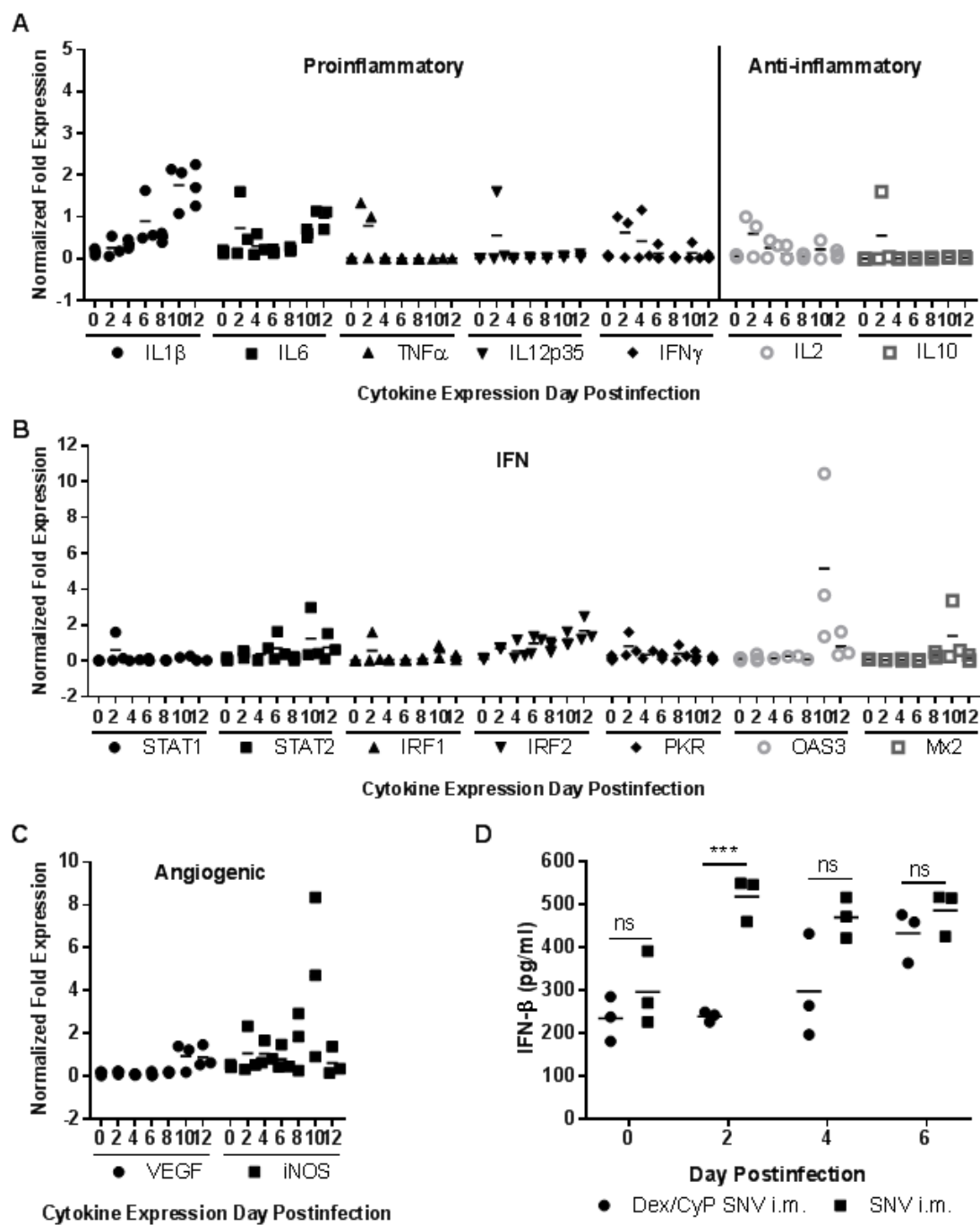
531 Figure 2



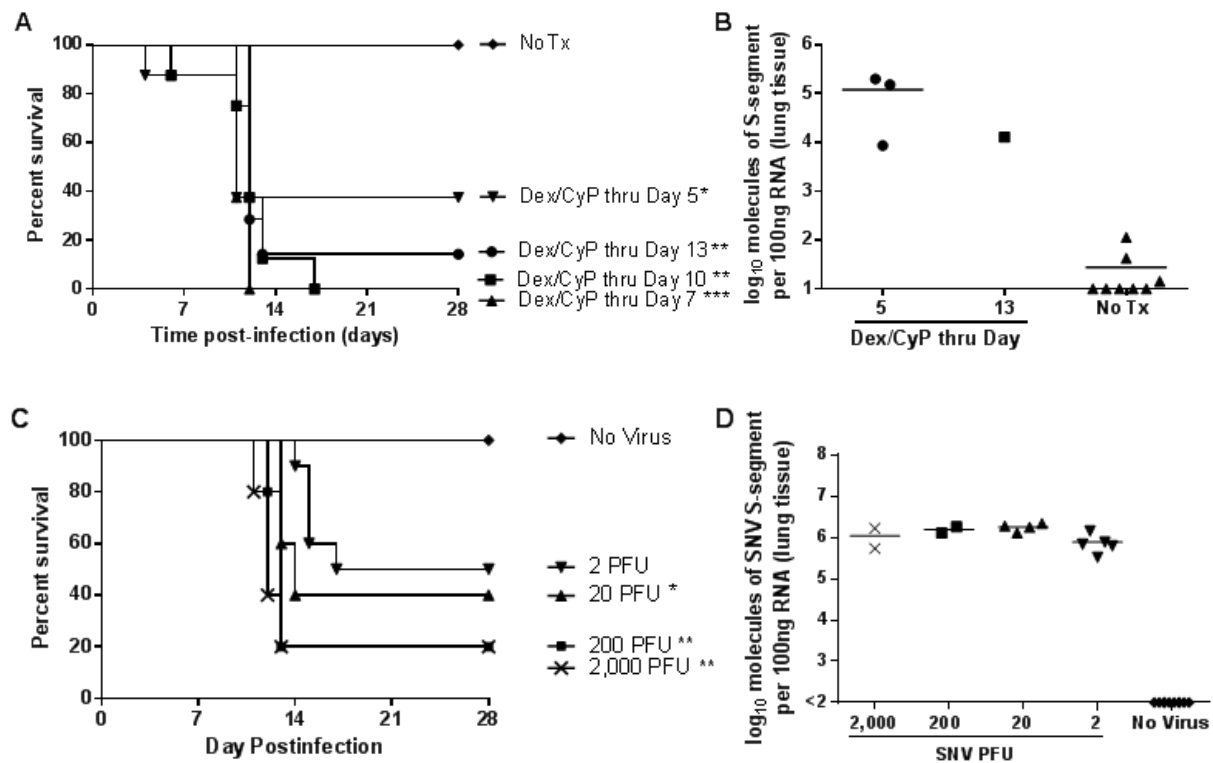
532

533

Figure 3



537 Figure 4



538

539

Figure 5

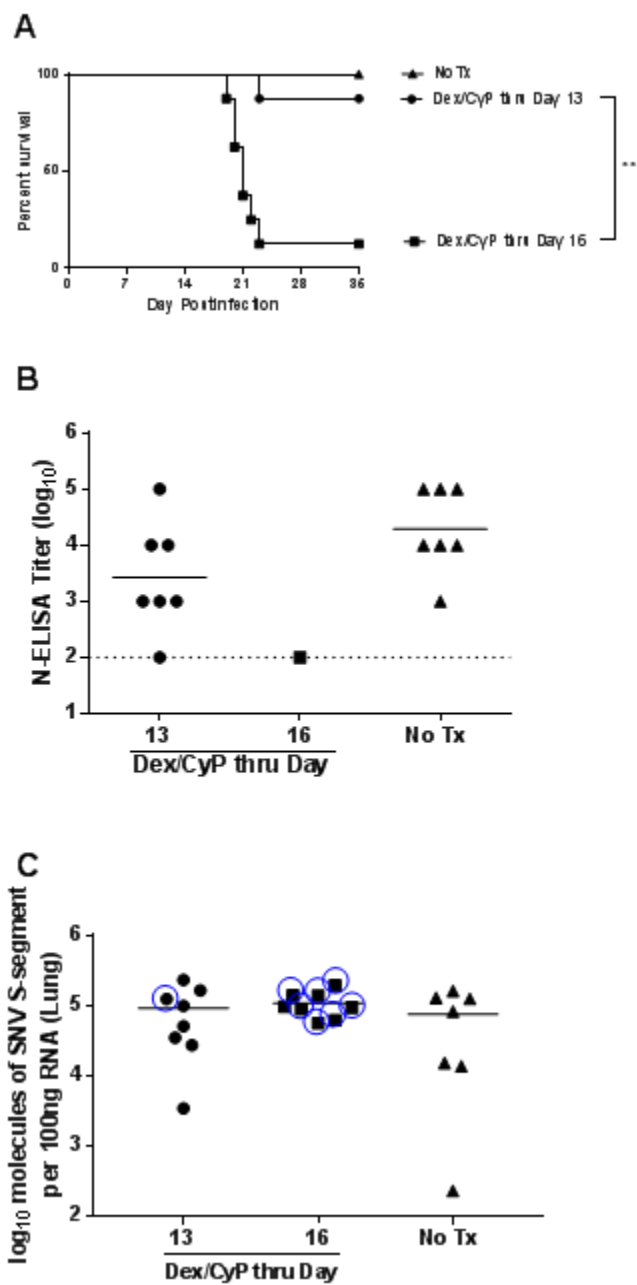


Figure 6

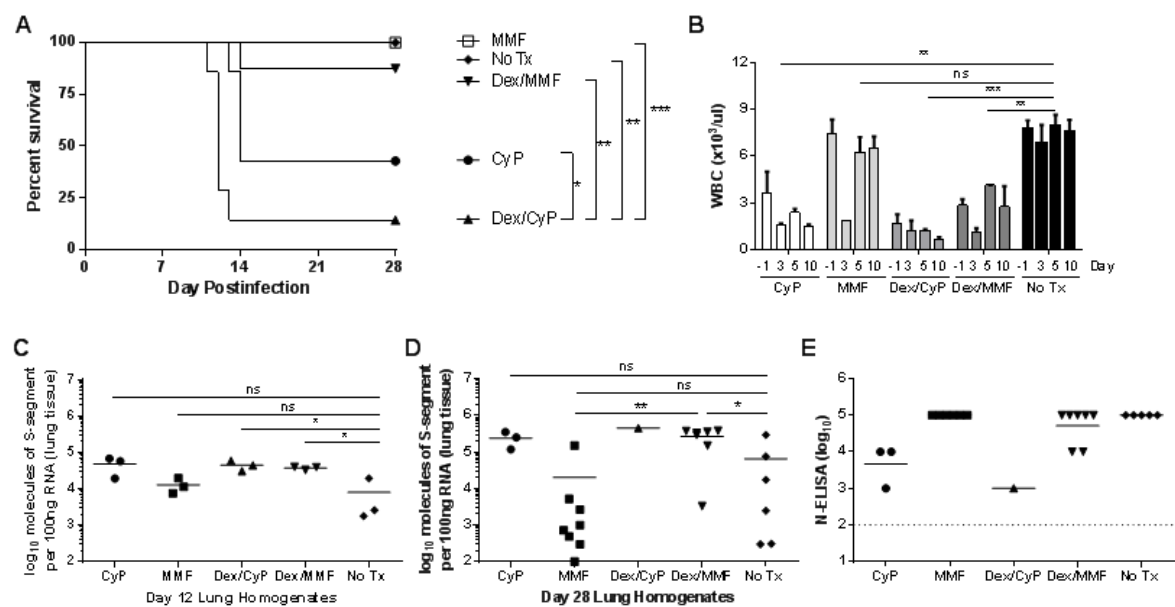
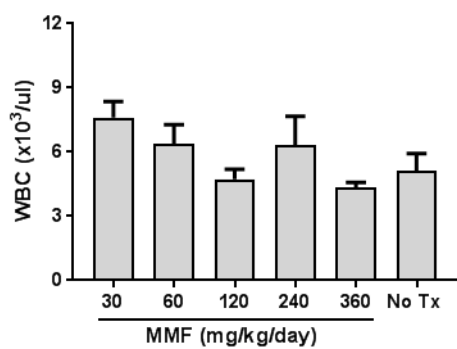


Figure 7



551 **Table S1.** Histologic findings in Dex/CyP SNV i.m., SNV i.n., and uninfected hamsters.

Dex/CyP SNV i.m. Day Postinfection	Hamster Organ				
	Lung Histologic Finding: Interstitial Inflammation	Kidney Histologic Finding	Liver Histologic Finding	Spleen Histologic Finding: Red Pulp Granulocytosis	Heart Histologic Finding: Myocardial Degeneration/Necrosis
0	-	-	-	-	-
2	-	-	-	-	+
4	-	-	-	-	-
6	++	-	-	++	-
8	+	-	-	-	-
10	++++	-	-	-	-
12	++	-	-	-	-

Dex/CyP SNV i.n. Day Postinfection	Lung Histologic Finding: Interstitial Inflammation	Kidney Histologic Finding	Liver Histologic Finding	Spleen Histologic Finding: Red Pulp Granulocytosis	Heart Histologic Finding: Myocardial Degeneration/Necrosis
0	-	-	-	-	-
2	-	-	-	-	+
4	-	-	-	-	+
6	-	-	-	+	-
8	+	-	-	+	-
10	+	-	-	-	-
12	+	-	-	-	-
14	++	-	-	-	-
16	++	-	-	-	++
18	++++	-	-	-	-
20	+++	-	-	-	-
22	+++	-	-	-	-

Dex/CyP No Virus Day Postinfection	Lung Histologic Finding: Interstitial Inflammation	Kidney Histologic Finding	Liver Histologic Finding	Spleen Histologic Finding: Red Pulp Granulocytosis	Heart Histologic Finding: Myocardial Degeneration/Necrosis
0	-	-	-	-	-
2	-	-	-	-	++
4	-	-	-	-	-
6	+	-	-	-	+
8	ND	-	-	+	-
10	-	-	-	-	-
12	+	-	-	+	-

552 Histopathological findings were scored as follows: +, very mild; ++, mild; +++, moderate; +++++, marked; ++++++, severe; -, negative or minimal finding. ND, no data due to autolysis of tissue.

553